



1

On the reflectance spectroscopy of snow

2

Alexander Kokhanovsky(1), Maxim Lamare(2,3), Biagio Di Mauro(4), Ghislain Picard

3

(2), Laurent Arnaud (2), Marie Dumont (3), François Tuzet (3,2), Carsten Brockmann(5),

4

Jason E. Box(6)

5

6

(1) VITROCISSET, Bratustrasse 7, D-64293 Darmstadt, Germany

7

(2) UGA, CNRS, Institut des Géosciences de l'Environnement (IGE), UMR 5001,

8

Grenoble, 38041, France

9

(3) Meteo-France–CNRS, CNRM UMR 3589, Centre d'Etudes de la Neige, Grenoble,

10

France

11

(4) Department of Earth and Environmental Sciences, University of Milano-Bicocca, Piazza

12

della Scienza, 1 20126 Milan, Italy

13

(5) Brockmann Consult, Max Planck Strasse 2, Geesthacht, Germany

14

(6) Geological Survey of Denmark and Greenland (GEUS), Copenhagen, Denmark

15

16

Abstract

17

We propose a system of analytical equations to retrieve snow grain size and absorption

18

coefficient of pollutants from snow reflectance or snow albedo measurements in the visible

19

and near-infrared regions of the electromagnetic spectrum. It is assumed that ice grains and

20

impurities (e.g., dust, black and brown carbon) are externally mixed. The system of nonlinear

21

equations is solved analytically in the assumption that impurities influence registered spectra in

22

the visible and not at near-infrared (and vice versa for ice grains). The theory is validated using

23

spectral reflectance measurements and albedo of clean and polluted snow at various locations

24

(Antarctica Dome C, European Alps). The technique to derive the snow albedo (plane and

25

spherical) from reflectance measurements at a fixed observation geometry is proposed. The

26

technique also enables the simulation of hyperspectral snow reflectance measurements in the

27

broad spectral range from ultraviolet to the near-infrared for a given snow surface in the case,



28 if the actual measurements are performed at restricted number of wavelengths (2-4,
29 depending on the type of snow and the measurements system).

30

31

32 **1. Introduction**

33 The reflective properties of clean and polluted snow are of importance for various applications
34 including climate (Hansen and Nazarenko, 2007) and environmental pollution (Nazarenko et al.,
35 2017) studies. The spectral snow reflectance is usually studied in the framework of the radiative
36 transfer theory. The application of the numerical methods for the solution of the radiative
37 transfer equation for snow layers has been performed by Mishchenko et al. (1999), Stamnes et al.
38 (2011), and He et al. (2018) among others. The approximate solutions of the radiative transfer
39 equation useful for snow optics and spectroscopy applications have been developed by Warren
40 and Wiscombe (1980), Wiscombe and Warren (1980) and Kokhanovsky and Zege (2004). In this
41 work, we propose an analytical snow albedo and reflectance model, which can be used to derive
42 snow optical and microphysical properties using measurements at just one to four wavelengths in
43 the visible and near-infrared depending on the measurement system and type of snow. In
44 particular, we present the method for the determination of snow grain size, absorption Angström
45 coefficient and spectral absorption coefficient of impurities embedded in the snow matrix
46 assuming an external mixture of snow grains and impurities. A technique to derive the snow
47 albedo from reflectance measurements is also presented. The absorption and extinction of light
48 by snow grains is treated in the framework of a geometrical optical approximation. The
49 absorption coefficient of impurities is modeled using the Angström power law. All derivations
50 are performed in the framework of the asymptotic radiative transfer theory (see, e.g.,
51 Kokhanovsky and Zege, 2004, Zege et al., 2011).



52

53 2. Theory

54 2.1 The snow reflectance

55 The snow reflectance R (equal to unity for ideal white Lambertian reflectors) can be presented in
56 the following way using approximate asymptotic radiative transfer theory (Kokhanovsky and
57 Zege, 2004):

58

$$59 \quad R = r_s^x, \quad (1)$$

60 where $x = u(\mu_0)u(\mu)/R_0$, R_0 is the reflectance of a semi-infinite non-absorbing snow layer,

$$61 \quad u(\mu_0) = \frac{3}{7}(1 + 2\mu_0), \quad \mu_0 \text{ is the cosine of the solar zenith angle, } \mu \text{ is the cosine of the viewing}$$

62 zenith angle, r_s is the snow spherical albedo:

$$63 \quad r_s = e^{-y}, \quad (2)$$

64 where

$$65 \quad y = 4 \sqrt{\frac{\beta}{3(1-g)}}, \quad (3)$$

66 g is the asymmetry parameter, β is the probability of photon absorption defined as the ratio of

67 absorption κ_{abs} and extinction κ_{ext} coefficients:

$$68 \quad \beta = \frac{\kappa_{abs}}{\kappa_{ext}}, \quad (4)$$



69 where

$$70 \quad \kappa_{abs} = \kappa_{abs}^{ice} + \kappa_{abs}^{pol}. \quad (5)$$

71 The first and second term in Eq. (5) correspond to the ice grains and pollutants, respectively. We
72 assume that scattering of light by impurities is much smaller than that by ice grains and,
73 therefore (Kokhanovsky and Zege, 2004),

$$74 \quad \kappa_{ext} = \frac{3c}{d}. \quad (6)$$

75 Here, $d = 1.5\bar{V} / \bar{S}$ is the effective diameter of ice grains, \bar{V} is the average volume of grains, \bar{S}
76 is their average projected area averaged over all directions, equal to $\Sigma/4$ for convex particles in
77 random orientation, where Σ is the average surface area and c is the volumetric concentration of
78 the snow grains.

79 It follows as $\alpha d \rightarrow 0$ in the visible and near infrared (Kokhanovsky and Zege, 2004) that :

$$80 \quad \kappa_{abs}^{ice} = A\alpha c, \quad (7)$$

81 where A is the grain shape-dependent parameter and $\alpha = \frac{4\pi\chi}{\lambda}$, where χ is the imaginary part of
82 the ice refractive index at the wavelength λ .

83 We present the absorption coefficient of pollutants in snow as

$$84 \quad \kappa_{abs}^{pol}(\lambda) = \kappa_0 \tilde{\lambda}^{-m}, \quad (8)$$

85 where $\kappa_0 \equiv \sigma_{abs}^{pol}(\lambda_0)$, $\tilde{\lambda} = \lambda / \lambda_0$. We will assume that $\lambda_0 = 1 \mu m$.



86 It follows from Eqs. (4)-(8):

$$87 \quad \beta = \frac{A\alpha d}{3} + \beta^{pol}, \quad (9)$$

88 where

$$89 \quad \beta^{pol} = \frac{\kappa_0 \tilde{\lambda}^{-m} d}{3c} \quad (10)$$

90 and therefore:

$$91 \quad y = \frac{4}{3} \sqrt{\frac{(A\alpha + \kappa_0 \tilde{\lambda}^{-m} c^{-1})d}{1-g}}. \quad (11)$$

92 Let the parameter $z = y^2$, from which it follows that:

$$93 \quad z = (\alpha + f \tilde{\lambda}^{-m})l, \quad (12)$$

94 where

$$95 \quad f = \frac{\kappa_0^*}{A} \quad (13)$$

96 $\kappa_0^* = \kappa_0 / c$ and

$$97 \quad l = \xi d \quad (14)$$

98 is the effective absorption length (EAL) and

$$99 \quad \xi = \frac{16A}{9(1-g)} \quad (15)$$

100 is a grain shape (but not the grain size) dependent parameter.

101 The parameter l can be determined directly from reflectance or albedo measurements, enabling

102 also the determination of the grain diameter $d = l / \xi$ assuming a particular shape of grains. It has



103 been found that the asymmetry parameter of crystalline clouds is usually in the range 0.74-0.76
 104 in the visible (Garret, 2008). The asymmetry parameter g for snow has not been measured before
 105 but we shall assume that it is close to that in crystalline clouds and adopt the value 0.75. It
 106 follows from experimental studies of Libois et al. (2014) that $A=1.6$ on average. Therefore, it
 107 follows (see Eq. 15): $\xi \approx 11.38$.

108 Using the EAL l , equations for the snow reflectance and spherical albedo may be simplified as:

$$109 \quad R = R_0 \exp(-x\sqrt{(\alpha + f\tilde{\lambda}^{-m})l}), \quad (16)$$

$$110 \quad r_s = \exp(-\sqrt{(\alpha + f\tilde{\lambda}^{-m})l}). \quad (17)$$

111 The plane albedo can be derived as well (Kokhanovsky and Zege, 2004):

$$112 \quad r = \exp(-u(\mu_0)\sqrt{(\alpha + f\tilde{\lambda}^{-m})l}). \quad (18)$$

113 The relationship between the albedo and the reflectance R can be found elsewhere (Kokhanovsky
 114 and Zege, 2004). It follows from Eq. (16) that the spectral reflectance of polluted snow is
 115 determined by four parameters: l, R_0, f, m . They can be estimated from the measurements of
 116 reflectance at four wavelengths. This also enables the determination of the spectral reflectance
 117 (and albedo, see Eq.(18)) at the visible and near – infrared wavelengths at an arbitrary λ . It
 118 follows:

$$119 \quad R_1 = R_0 \exp(-x\sqrt{(\alpha_1 + f\tilde{\lambda}_1^{-m})l}), \quad (19)$$

$$120 \quad R_2 = R_0 \exp(-x\sqrt{(\alpha_2 + f\tilde{\lambda}_2^{-m})l}) \quad (20)$$

$$121 \quad R_3 = R_0 \exp(-x\sqrt{(\alpha_3 + f\tilde{\lambda}_3^{-m})l}) \quad (21)$$



122
$$R_4 = R_0 \exp(-x\sqrt{(\alpha_4 + f\tilde{\lambda}_4^{-m})}l) \quad (22)$$

123 where the numbers 1, 2, 3, and 4 signify the wavelengths used. Equations (19)-(22) can be used
 124 to compute four unknown parameters given above, and, therefore, determine reflectance and
 125 albedo at any wavelength in the visible and the near-infrared using Eqs. (16)-(18). Let us assume
 126 that the spectral channels are selected in a way that the effects of ice absorption can be neglected
 127 in the first two channels (λ_1, λ_2) and effects of absorption by pollutants are negligible in the
 128 second pair of channels (λ_3, λ_4). This situation is typical of not heavily polluted snow. Then it
 129 follows instead of Eqs. (19)-(22):

130
$$R_1 = R_0 \exp(-x\sqrt{f\tilde{\lambda}_1^{-m}}l), \quad (23)$$

131
$$R_2 = R_0 \exp(-x\sqrt{f\tilde{\lambda}_2^{-m}}l), \quad (24)$$

132
$$R_3 = R_0 \exp(-x\sqrt{\alpha_3}l), \quad (25)$$

133
$$R_4 = R_0 \exp(-x\sqrt{\alpha_4}l). \quad (26)$$

134 Eqs. (25), (26) can be used to find the pair (l, R_0):

135
$$R_0 = R_3^{\varepsilon_1} R_4^{\varepsilon_2}, \quad l = \frac{1}{x^2 \alpha_4} \ln^2 \left[\frac{R_4}{R_0} \right], \quad (27)$$

136 where $\varepsilon_1 = 1/(1-b)$, $\varepsilon_2 = 1/(1-b^{-1})$, $b = \sqrt{\alpha_3/\alpha_4}$. Then it follows from Eqs. (23), (24) that:

137
$$m = \frac{\ln(p_1/p_2)}{\ln(\lambda_2/\lambda_1)}, \quad (28)$$



138
$$f = \frac{p_1 \tilde{\lambda}_1^m}{x^2 l}, \quad (29)$$

139 where $p_k = \ln^2(R_k / R_0)$. In case of the absence of pollutants, Eqs. (27) remain valid. However,
140 the parameters m and f are undefined and $R = R_0 \exp(-x\sqrt{al})$.

141 One may also derive the impurity absorption coefficient at the wavelength
142 λ_0 normalized to the concentration of ice grains c (see Eq. (13)):

143
$$\kappa_0^* = Af, \quad (30)$$

144 where f is given by Eq.(29). The normalized absorption coefficient at each wavelength can also
145 be found using Eqs. (8), (28), (30).

146 To determine the concentration of pollutants (c_p) one must either know in advance or determine
147 the impurity volumetric absorption coefficient defined as:

148
$$K(\lambda_0) = \frac{\bar{C}_{abs}(\lambda_0)}{\bar{V}}, \quad (31)$$

149 where \bar{C}_{abs} is the average absorption cross section of impurities and \bar{V} is the average volume of absorbing
150 impurities. Namely, it follows by definition:

151
$$c_p = \frac{\kappa_0}{K(\lambda_0)} \quad (32)$$

152 and



153
$$\mathbb{C} = \frac{K_0^*}{K(\lambda_0)}, \quad (33)$$

154 where $\mathbb{C} = c_p / c$.

155 The value of $K(\lambda_0)$ can be found, if one knows the type of pollutants and their microphysical properties.

156 In particular, it follows for the impurities much smaller than the wavelength λ_0 (van de Hulst, 1981) that :

157
$$K(\lambda_0) = F \alpha_{pol}(\lambda_0), \quad (34)$$

158 where

159
$$\alpha_{pol}(\lambda_0) = \frac{4\pi\chi_{pol}(\lambda_0)}{\lambda_0} \quad (35)$$

160 is the pollutant bulk absorption coefficient, $\chi_{pol}(\lambda_0)$ is the imaginary part of pollutant refractive

161 index and n_{pol} is the real part of the pollutant refractive index,

162
$$F = \frac{9n_{pol}}{(n_{pol}^2 + 1 - \chi_{pol}^2)^2 + 4n_{pol}^2\chi_{pol}^2}. \quad (36)$$

163 It follows that $F = 0.9$ for soot (assuming that $n=1.75$, $\chi_{pol} = 0.47$ in the visible). One can see

164 that \mathbb{C} can be found if one knows the refractive index of absorbing Rayleigh particles in

165 advance.

166

In particular, it follows for soot impurities that:

167
$$\mathbb{C} = \frac{Ap_1\tilde{\lambda}_1^m}{x^2IF\alpha_{pol}(\lambda_0)}. \quad (37)$$



168 In case of non-Rayleigh scatterers, one needs to know not only the refractive index but
 169 also the particle size distribution and shape of particles, enabling the determination of the
 170 impurity volumetric absorption coefficient $K(\lambda_0)$ and, therefore, the normalized concentration
 171 of impurities

$$172 \quad \mathbb{C} = \frac{A p_1 \tilde{\lambda}_1^m}{x^2 l K(\lambda_0)}. \quad (38)$$

173

2.2. The snow albedo

174 In case if the plane albedo is the measured physical quantity one needs to find only three
 175 constants: l, f, m .

176 The respective analytical equations can be presented as:

$$177 \quad r_1 = \exp(-u(\mu_0) \sqrt{(\alpha_1 + f \tilde{\lambda}_1^{-m}) l}), \quad (39)$$

$$178 \quad r_2 = \exp(-u(\mu_0) \sqrt{(\alpha_2 + f \tilde{\lambda}_2^{-m}) l}), \quad (40)$$

$$179 \quad r_3 = \exp(-u(\mu_0) \sqrt{(\alpha_3 + f \tilde{\lambda}_3^{-m}) l}). \quad (41)$$

180 We shall assume that the last channel is not influenced by impurities and the first two channels
 181 are not influenced by the absorption of light by grains. Then it follows that:

$$182 \quad r_1 = \exp(-u(\mu_0) \sqrt{f \tilde{\lambda}_1^{-m} l}), \quad (42)$$

$$183 \quad r_2 = \exp(-u(\mu_0) \sqrt{f \tilde{\lambda}_2^{-m} l}), \quad (43)$$



$$184 \quad r_3 = \exp(-u(\mu_0)\sqrt{\alpha_3 l}). \quad (44)$$

185 The EAL can be found from Eq. (44):

$$186 \quad l = \frac{\ln^2 r_3}{u^2(\mu_0)\alpha_3}. \quad (45)$$

187 It follows from Eqs. (42), (43) that:

$$188 \quad m = \frac{\ln(\psi_2 / \psi_1)}{\ln(\lambda_1 / \lambda_2)}, f = \frac{\psi_1 \tilde{\lambda}_1^m}{u^2(\mu_0)l}, \quad (46)$$

189 where $\psi_k = \ln^2 r_k$.

190 In case of unpolluted snow, one derives:

$$191 \quad r = \exp(-u(\mu_0)\sqrt{\alpha l}). \quad (47)$$

192 Eq. (45) can be used to find the effective absorption length and, therefore, the spectral albedo of
193 unpolluted snow at any wavelength using Eq. (47).

194 One can derive from Eq. (45):

$$195 \quad \sigma_l = \nu \sigma_{r_3}, \quad \nu = \frac{2}{\ln r_3}, \quad (48)$$

196 where σ_l is the relative error in the determination of the effective absorption length and σ_{r_3} is the relative
197 error of the plane albedo measurement at the wavelength λ_3 . Taking into account that $\ln r_3 \leq 0$,

198 one concludes that the positive bias of the measured plane albedo will lead to the
199 underestimation of the effective absorption length (and, therefore, snow grain size) with the



200 enhancement coefficient ν . The enhancement coefficient is larger for larger values of albedo (smaller particles
201 or shorter wavelengths). Similar analysis for the concentration of pollutants is more involved because
202 the errors of measurements at three channels influence the concentration of pollutants determination.
203 In particular, one finds that the positive bias in the measured albedo in the visible will lead to the
204 underestimation of the concentration of pollutants (assuming that the grain size is exactly
205 known). It should be pointed out that in most cases the concentration of pollutants is so small
206 that it can not be assessed using optical instruments (change in reflectance is inside experimental
207 measurement error). This issue has been discussed by Zege et al. (2011) and Warren (2013).
208 Similar conclusions hold also if the reflectance (and not albedo) is the measured quantity.

208 3. Experiment

209 3.1 The measurements of the plane albedo

210 We have applied the technique developed above to the measured spectral plane albedo both for
211 polluted and pure snow. Therefore, in-situ spectral albedo measurements were obtained from two
212 different field sites located in Antarctica (clean snow) and the French Alps (polluted snow).

213 *The spectral albedo of pure snow* (very low amount of impurities) was measured at Dome C
214 (75°5' S, 123°17' E), in Antarctica using an automated spectral radiometer (Libois et al., 2015;
215 Picard et al., 2016; Dumont et al., 2017). The instrument is composed of two individual heads
216 located approximately 1.5 m above the surface. Each head contains two cosine receptors facing
217 upward and downward, which receive the incident solar radiation and the reflected radiation. The
218 collectors are connected to a MAYA2000 PRO Ocean Optics spectrometer with fibre optics



219 through an optical switch. Radiation is measured over 350-2500 nm spectral range with an
220 effective spectral resolution of 3 nm. Albedo was calculated as the ratio of the upward and
221 downward spectral irradiance. The full description of the instrument and the processing steps to
222 calculate the spectral albedo are given by Picard et al. (2016). The spectral albedo measurements
223 used here were made on the 10th January 2017, with a solar zenith angle of 63.2°, during clear
224 sky conditions assessed by ground observations.

225 *The spectral albedo of a spring alpine snowpack* was measured at the Col du Lautaret field site
226 (45°2' N, 6°2' E, 2100 m a.s.l.) in the French Alps. The measurements were performed using a
227 non-automated version of the spectrometer system described above. The hand-held instrument
228 has a single light collector, located at the end of 3 m boom placed 1.5 m above the surface. The
229 boom is rotated by the operator to successively acquire the downward and upward solar
230 radiation. Five spectral albedo measurements were obtained on 12th April, 2017 across a 100 m
231 transect, in attempt to account for spatial variability. The measurements were acquired in clear
232 sky conditions, with a solar zenith angle varying between 47.9° and 52.2°. The five spectral
233 albedo measurements were averaged for the comparison with the theory.

234 The results of inter-comparison of measurements and the theory presented above are illustrated
235 in Fig.1. The parameters l, f, m have been found from Eqs. (42)-(44) and the measurements at
236 the wavelengths $\lambda_1 = 400nm, \lambda_2 = 560nm, \lambda_3 = 1020nm$. At all measurement sites the results of
237 the inter-comparison are excellent and similar to that presented in Fig.1. Therefore, the theory
238 can be used to derive snow optical and microphysical properties even for polluted snowpack.
239 The derived spectral probability of photon absorption for the case shown in Fig. 1 is presented in
240 Fig.2. The derived absorption coefficient (assuming $c=1/3$), the grain diameter and the
241 absorption Angström parameter for five samples are listed in Table 1 (lines 1-5). It follows that



242 the value of m is in the range 2.4 - 4.1 consistent with the identified presence of dust particles in
243 snow (Doherty et al., 2010). The pure black carbon impurities have the values of m close to one.
244 The grain diameter is in the range 1.5-1.9 mm consistent with low values of snow albedo at
245 1020nm (see Fig.1). The results of the application of the technique to the pure snow (no
246 pollution) albedo measured in Antarctica are illustrated in Fig.3. One can see that the agreement
247 is excellent and the value of snow albedo depends just on one parameter – the characteristic
248 length, which has been derived at a single wavelength (1020nm). The derived grain diameter for
249 the case presented in Fig.3 is equal to 0.5mm.

250

251 **3.2 The measurements of the spectral reflectance**

252 The application of the developed theory to the measurements of the spectral reflectance is
253 presented in Fig.4 for two locations with different dust load (39.6ppm and 107.4ppm). The
254 spectral reflectance of snow was measured in the European Alps (45°55'56.70"N;
255 45°55'56.70"N) at the solar zenith angle equal to 52 degrees. The measurements were made on
256 March 14th 2014, after a major transport and deposition of mineral dust from the Saharan desert.
257 The event was very intense, and it was reported in the recent scientific literature regarding snow
258 optical properties, (Di Mauro et al., 2015; Dumont et al., 2017), atmospheric chemistry and
259 physics (Belosi et al., 2017), and also microbiology (Weil et al., 2017). The dust transport event
260 deposited fine mineral dust particles from the atmosphere via wet deposition, according to the
261 BSC-DREAM-8b model (Basart et al., 2012). Spectral measurements of snow were made using a
262 field spectrometer (Field Spec Pro, Analytical Spectral Devices, ASD). This instrument features
263 a spectral range of 350-2500 nm, a full width at half maximum of 5–10 nm, and a spectral



264 resolution of 1 nm. Data presented here were collected under clear sky conditions at noon.
265 Incident radiation was estimated using a Lambertian Spectralon panel. Reflected radiance was
266 divided by incident radiance, and the hemispherical conical reflectance factor (HCRF) was
267 calculated for three plots containing 0.92, 39.6 and 107.4 ppm of dust. Dust concentration was
268 measured with a Coulter Counter by integrating particles with a diameter smaller than 18 μm .
269 Spectral measurements were performed at nadir using a bare optical fiber (field of view of 25°)
270 at 80 cm from the snow sample. Both the optical fiber and the spectralon panel were equipped
271 with an optical level. Further details on this dataset can be found in Di Mauro et al. (2015).

272 One can see that the theory works well not only for the albedo measurements (see the
273 previous section) but also for the reflectance measurements for polluted snow layers. In
274 particular, our results are closer to the measurements as compared to the theoretical model
275 described by Flanner et al. (2007) (see Fig.4b in Di Mauro et al., 2015). The derived parameters
276 are given in Table 1 (lines 6-7). The value of m is 4.1 for the first case and it is 6.4 for the second
277 case with high dust concentration. Because the difference is quite large for the close locations we
278 conclude that snow also contained other pollutants (say, soot) and the determined value of m
279 represents the combined effect with larger values of m for larger concentrations of dust, which is
280 consistent with other observations of this parameter in snow (Doherty et al., 2010). The retrieved
281 absorption coefficient of snow pollutants (at the wavelength $\lambda^* = 560\text{nm}$) is 0.1191 m^{-1} for the
282 dust concentration 39.6ppm and it is 0.3123 m^{-1} for the dust concentration of 107.4 ppm.
283 Assuming that the dust chemical composition and also the dust particle size distribution are the
284 same at both locations we can assume that the ratio of absorption coefficients at two locations
285 should be equal to the ratio of dust concentrations. This is really so with the difference just 3%



286 which is within the accuracy of experimental measurements. The mass absorption coefficient can
287 be estimated using:

$$288 \quad K_m = \frac{\kappa_{abs}^{pol}(\lambda^*)}{\mathbb{C}\rho c}, \quad (49)$$

289 where ρ is the density of the substance of impurities. Assuming that:

$$290 \quad \rho = 2.62 \text{ g / cm}^3 \text{ (as for quartz)}, c = 1/3, \mathbb{C} = 107.4 \text{ ppm and } \kappa_{abs}^{pol}(\lambda^*) = 0.3123 \text{ m}^{-1}, \quad (50)$$

291 one can derive that:

$$292 \quad K_m = 0.0033 \text{ m}^2 / \text{g}, \quad (51)$$

293 which is consistent with the values of MAC given by Utry et al.(2015) (e.g.,

294 $0.0023 \text{ m}^2 / \text{g}$ for quartz and $0.0051 \text{ m}^2 / \text{g}$ for illite (see their Table 1)).

295

296 **4. Conclusions**

297 In this work, we have presented a sequence of analytical equations, which can be used to
298 determine the snow grain size, the absorption coefficient of impurities, and the absorption
299 Angström coefficient of surface snow impurities from the snow reflectance measured at four
300 wavelengths. Two of them are located in the visible and two - in the near infrared as suggested
301 by Warren (2013). In principle, the refractive index of dust and dust size distribution can be also
302 determined using derived spectral absorption coefficient of dust and assuming the shape of dust
303 particles. However, we did not make an attempt for such retrievals in this work. The method for



304 the retrieval of the complex refractive index and single scattering optical properties of dust
305 deposited in mountain snow based on exact radiative transfer calculations has been proposed by
306 McKenzie Siles et al. (2016) in the assumption that local optical properties of dust grains can be
307 simulated assuming the spherical shape of particles. Their method is based on the extraction of
308 dust grains from snowpack. Our technique does not require such a complicated procedure.

309 We have demonstrated how snow albedo can be derived from spectral reflectance measurements
310 avoiding complicated integration with respect to the observation geometry (azimuth, viewing
311 angle). The last point is useful for the determination of the snow *albedo* from spectral *reflectance*
312 measurements (say, from aircraft or satellite) at a fixed observation geometry. Although the
313 comprehensive validation of the retrievals has not been attempted, we have found that the ratio
314 of derived absorption coefficients of pollutants at two concentrations is close to the ratio of
315 pollutant concentrations derived independently, which indeed should be the case taking the
316 proximity of two measurement sites with different dust loads. The general validity of the
317 approach is proven using field measurements (Alps, Antarctica) of both spectral reflectance and
318 plane albedo.

319 The determination of the effective absorption length l (unlike the effective grain diameter d)
320 both from reflectance and albedo measurements is practically insensitive to *a priori* unknown
321 shape of ice crystals. Therefore, this length may be useful for the characterization of snowpack
322 microstructure (in addition to the grain size d). The results presented in this work are useful for
323 the interpretation of snow properties using both reflectance spectroscopy (Hapke, 2005) and
324 imaging spectrometry (Dozier et al., 2009).

325



326 **5. Acknowledgments**

327 This work was mainly supported by the European Space Agency in the framework of ESRIN
328 contract No. 4000118926/16/I-NB “Scientific Exploitation of Operational Missions (SEOM)
329 Sentinel-3 Snow (Sentinel-3 for Science, Land Study 1: Snow)”. CNRM/CEN and IGE are part of
330 labex OSUG@2020. Measurements in the French Alps were funded by the ANRJJC grant EBONI
331 16-CE01-0006 and at Dome C by ANR JCJC MONISNOW 1-JS56-005-01.

332



333 **References**

- 334 S. Basart, S., C. Pérez, S. Nickovic, E. Cuevas, and J. M. Baldasano, "Development and
335 evaluation of the BSC-DREAM8b dust regional model over Northern Africa, the Mediterranean
336 and the Middle East", *Tellus B*, vol. 64, 2012, doi:10.3402/tellusb.v64i0.18539, 2012.
- 337 F. Belosi, M. Rinaldi, S. Decesari, L. Tarozzi, A. Nicosia, A., and G. Santachiara, "Ground
338 level ice nuclei particle measurements including Saharan dust events at a Po Valley rural site
339 (San Pietro Capofiume, Italy)", *Atmospheric Research*, vol. 186, pp. 116–126,
340 <https://doi.org/10.1016/J.ATMOSRES.2016.11.012>, 2017.
- 341 B. Di Mauro, F. Fava, L. Ferrero, R. Garzonio, G. Baccolo, B. Delmonte, and R. Colombo,
342 "Mineral dust impact on snow radiative properties in the European Alps combining ground,
343 UAV, and satellite observations", *J. Geophys. Res. Atmos.*, vol. 120, pp. 6080–6097,
344 doi:10.1002/2015JD023287, 2015.
- 345 S. J. Doherty, S. G. Warren, T. C. Grenfell, A. D. Clarke, and R. E. Brandt, "Light-absorbing
346 impurities in Arctic snow", *Atmos. Chem. Phys.*, vol. 10, 11647–11680, 2010.
- 347 J. Dozier, R. O. Green, A. W. Nolin, and T. H. Painter, "Interpretation of snow properties from
348 imaging spectrometry", *Remote Sens. Env.*, vol. 113, pp. S25–S37, 2009.
- 349 M. Dumont, L. Arnaud, G. Picard, Q. Libois, Y. Lejeune, P. Nabat, and S. Morin, S. "In situ
350 continuous visible and near-infrared spectroscopy of an alpine snowpack". *The Cryosphere*,
351 vol. 11, N3, pp. 1091–1110, <https://doi.org/10.5194/tc-11-1091-2017>, 2017.



- 352 M. G. Flanner, C. S. Zender, J. T. Randerson, and P. J. Rash, "Present – day climate forcing and
353 response from black carbon in snow", *J. Geophys. Res Atmos.*, vol.112, D11202, doi:
354 10.1029/2006JD008003, 2007.
- 355 T. J. Garrett, "Observational quantification of the optical properties of cirrus cloud", *Light*
356 *Scattering Reviews* (ed. by A. Kokhanovsky), 3, 1-26, Praxis-Springer, 2008.
- 357 J. Hansen, and L. Nazarenko, 2004: "Soot climate forcing via snow and ice albedos", *Proc.*
358 *Natl. Acad. Sci.*, 101, 423-428, doi:10.1073/pnas.2237157100, 2004.
- 359 B. Hapke, *Theory of reflectance and emittance spectroscopy*, Cambridge: Cambridge University
360 Press, 2005.
- 361 C. He, K.-N. Liou, Y. Takano, P. Yang, L. Qi, and F. Chen, "Impact of grain shape and multiple
362 black carbon internal mixing on snow albedo: parameterization and radiative effect analysis", *J.*
363 *Geophys. Res.*, 123, 1253-1268, 2018.
- 364 A. A. Kokhanovsky, E.P. Zege, "Scattering optics of snow", *Appl. Optics*, vol. 43, N7, pp.1589-
365 1602, 2004.
- 366 Q. Libois, G. Picard, M. Dumont, L. Arnaud, C. Sergent, E. Pougatch, M. Sudul, and D. Vial, "
367 Experimental determination of the absorption enhancement parameter of snow", *J. Glaciology*,
368 60, N 222, 2014.
- 369 Q. Libois, G. Picard, L. Arnaud, M. Dumont, M. Lafaysse, S. Morin, and E.
370 Lefebvre, "Summertime Evolution of Snow Specific Surface Area close to the Surface on the
371 Antarctic Plateau," *The Cryosphere*, 9, N6, 2383-2398, 2015.
- 372 S. McKenzie Skiles, T. Painter, G. S. Okin, "A method to retrieve the spectral complex refractive



- 373 index and single scattering optical properties of dust deposited in mountain snow”, J.
374 Glaciology, 63, N237, 133-147.
- 375 M. I. Mishchenko, J.M. Dlugach, E.G. Yanovitskij, and N.T. Zakharova, ”Bidirectional
376 reflectance of flat, optically thick particulate layers: An efficient radiative transfer solution and
377 applications to snow and soil surfaces”, *J. Quant. Spectrosc. Radiat. Transfer*, vol. 63, pp. 409-
378 432, doi:10.1016/S0022-4073(99)00028-X, 1999.
- 379 Y. Nazarenko, S. Fournier, U. Kurien, R. B. Rangel-Alvarado, O. Nepotchatykh, P. Seers, P. A.
380 Ariya, ”Role of snow in the fate of gaseous and particulate exhaust pollutants from gasoline-
381 powered vehicles”. *Environmental Pollution*, 223, 665 DOI: 10.1016/j.envpol.2017.01.082,
382 2017
- 383 G. Picard, Q. Libois, L. Arnaud, G. Verin, and M. Dumont, “Development and calibration of an
384 automatic spectral albedometer to estimate near-surface snow SSA time series.” *The
385 Cryosphere*, 10, N3, 1297-1316, 2016.
- 386 K. Stamnes, B. Hamre, J. J. Stamnes, G. Ryzikov, C. Biryulina, R. Mahoney, B. Haus, and A.
387 Sei, ”Modeling of radiation transport in coupled atmosphere-snow-ice-ocean systems”, *J.
388 Quant. Spectrosc. Radiat. Transfer*, 112, 714-726, 2011.
- 389 N. Utry, T. Ajtai, M. Pinter, E. Tombacz, E. Illes, Z. Bozoki, and G. Szabo, ”Mass-specific
390 optical absorption coefficients and imaginary part of the complex refractive indices of mineral
391 dust components measured by a multi-wavelength photoacoustic spectrometer”, *Atmos. Meas.
392 Techniques*, 8, 401-410, 2015.
- 393 H. C. Van de Hulst, *Light scattering by small particles*, N.Y: Dover, 1981.



394 S. G. Warren, W. J. Wiscombe, "A model for spectral albedo of snow: II. Snow containin
395 atmospheric aerosols", *J. Atmos. Sci.*, vol. 37, pp. 2734-2745, 1980.

396 S. G. Warren, "Can black carbon in snow be detected by remote sensing", *J. Geophys. Res.*,
397 *Atmospheres*, 118, 779-786.

398 T. Weil, C. De Filippo, D. Albanese, C. Donati, M. Pindo, L. Pavarini, and F. Miglietta, "Legal
399 immigrants: invasion of alien microbial communities during winter occurring desert dust
400 storms", *Microbiome*, vol. 5, No 1, <https://doi.org/10.1186/s40168-017-0249-7>, 2017.

401 W. J. Wiscombe, and S. G. Warren, "A model for spectral albedo of snow: I. Pure snow", *J.*
402 *Atmos. Sci.*, vol. 37, pp. 2712-2733.

403 E. P. Zege, I. L. Katsev, A. V. Malinka, A. S. Prikhach, G. Heygster, and H. Wiebe, "Algorithm
404 for retrieval of the effective snow grain size and pollutants amount from satellite
405 measurements", *Rem. Sens. Env.*, 115, 2674-2685.

406



407

408 Tables

409

410 Table 1. The derived snow parameters for the five samples. The value of c is assumed to be equal $1/3$,
 411 which leads to the extinction length ($l_{ext} = 1/\sigma_{ext}$) to be equal to the effective grain diameter d . The
 412 absorption coefficient is given at the wavelengths $\lambda_0=1000\text{nm}$ and $\lambda^* = 560\text{nm}$.

413	N	κ_0, m^{-1}	$\kappa_{abs}^{pol}(\lambda^*), m^{-1}$	m	d, mm
414	1	0.0182	0.1954	4.1	2.1
415	2	0.0342	0.2668	3.5	2.2
416	3	0.1073	0.7194	3.3	1.7
417	4	0.0769	0.5324	3.3	1.9
418	5	0.0943	0.3848	2.4	2.2
419	6	0.0111	0.1191	4.1	2.5
420	7	0.0077	0.3123	6.4	1.5

421

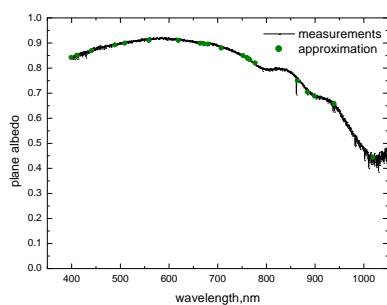
422

423



424

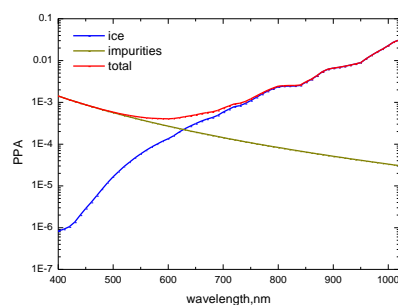
425 Figures



426

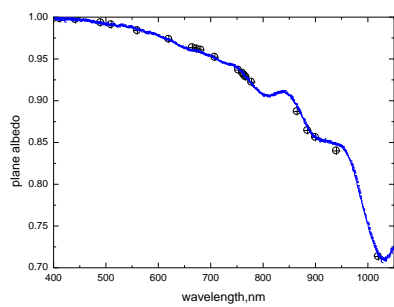
427 Fig.1. The intercomparison of theory (symbols) with experimental measurements of plane albedo
428 (line) performed in French Alps (45°2' N, 6°2' E, 2100 m *a.s.l.*) for the dust – loaded snowpack.
429 The parameters l , f , m have been derived from the measurements at 400, 560, and 1020nm.

430



431

432 Fig.2. The derived spectral probability of photon absorption for the case presented in Fig.1.



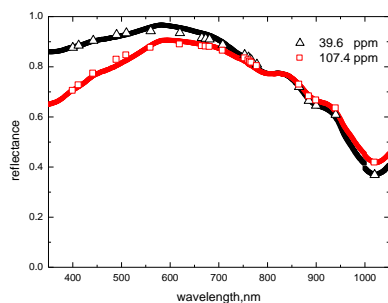
433

434 Fig.3 The inter-comparison of theory (symbols) with experimental measurements of plane albedo
435 (line) performed in Antarctica (Dome C, 75°5' S, 123°17' E) for pure snow. The parameters l , f ,
436 m have been derived from the measurements at 400, 560, and 1020nm.

437



438



439

440 Fig.4 The inter-comparison of theory (symbols) with experimental measurements (line) in
441 European Alps (45°55'56.70"N; 45°55'56.70"N) for the polluted snowpack. The parameters R_0 ,
442 l , f , m have been derived from the measurements at 400, 560, 865 and 1020nm.
443 Reflectance measurements were collected on snow containing different concentration of dust:
444 39.6 ppm (black line) and 107.4 ppm (red line). A complete description of this dataset is
445 presented in Di Mauro et al. (2015).

446

447

448